

Design and Analysis of a Wireless Nanosensor Network for Monitoring Human Lung Cells

Eisa Zarepour, Najmul Hassan, Mahbub Hassan, Chun Tung Chou
School of Computer Science and Engineering, University of New South Wales, Sydney, Australia
Email:{ezarepour, nhassan, mahbub, ctchou}@cse.unsw.edu.au

Majid Ebrahimi Warkiani
Laboratory of Microfluidics & Biomedical Microdevices, School of Mechanical and Manufacturing Engineering
University of New South Wales, Sydney Australia
Email:m.warkiani@unsw.edu.au

ABSTRACT

Thanks to nanotechnology, it is now possible to fabricate sensor nodes below 100 nanometers in size. Although wireless communication at this scale has not been successfully demonstrated yet, simulations confirm that these sensor nodes would be able to communicate in the terahertz band using graphene as a transmission antenna. These developments suggest that deployment of wireless nanoscale sensor networks (WNSNs) inside human body could be a reality one day. In this paper, we design and analyse a WNSN for monitoring human lung cells. We find that respiration, i.e., the periodic inhalation and exhalation of oxygen and carbon dioxide, is the major process that influences the terahertz channel inside lung cells. The channel is characterised as a two-state channel, where it periodically switches between good and bad states. Using real human respiratory data, we find that the channel absorbs terahertz signal much faster when it is in bad state compared to good state. Our simulation experiments confirm that we could reduce transmission power of the nanosensors, and hence the electromagnetic radiation inside lungs due to deployment of WNSN, by a factor of 20 if we could schedule all communication only during good channel states. We propose two duty cycling protocols along with a simple channel estimation algorithm that enables nanosensors to achieve such scheduling.

Keywords: WNSNs, Nanoscale communication, Health monitoring systems, Nannosensors, communication protocols.

1. INTRODUCTION

Recent advancements in nanotechnology has made it possible to fabricate sensor nodes below 100 nanometers in size using various types of novel materials. These nanosensors have extra-ordinary sensing capabilities and can sense a range of information at molecular level. For example, it is now possible to fabricate supersensitive nanoscale sensors

that can measure chemical compounds in concentrations as low as one part per billion [12]. Medical researchers are already considering use of nanoparticles for targeted delivery of drugs to infected cells within human body [3, 14]. When sensing is combined with these nanoparticles, they can also collect a range of valuable cell-level data for early detection of diseases. Wireless communication for such nanosensors will be a key enabler for such cell-level data collection from human body.

Although wireless communication at nanoscale has not been successfully demonstrated yet, recent simulation studies confirm that these nanosensors may be able to communicate in the terahertz band using graphene as a transmission antenna [7]. Following this development, in this paper, we present the design of a WNSN for monitoring human lung cells. The WNSN continuously measures important cell-level data inside lung cells and send them back to the Internet using terahertz communication.

The success of such WNSN will critically depend on the ability of the nanosensors to communicate reliably with other nanosensors to forward the data to a sink, which can directly communicate with a macro-scale receiver outside human body, such as a skin-patch. Electromagnetic radiation inside lungs due to wireless communication is another important consideration for such deployments. Hence, communication reliability must be achieved with as little transmission power as possible, which will minimise radiation. These requirements cannot be met without good knowledge of the channel characteristics. Thus the primary focus of this paper is to characterise the terahertz channel inside human lung.

It has been shown that terahertz is highly susceptible to molecular absorption, which can be characterised using radiative transfer theory [6, 18]. Essentially, this theory says that the amount of signal absorption will depend on the types of molecules are present in the channel, as different molecules have different absorption capabilities. We use this theory to study the characteristics of terahertz communication channels that may be encountered in human lungs. We have found that the respiration process is the major factor that influences the terahertz channel inside lung cells. The channel periodically switches between good state (i.e., bit error rate in the channel is low) and bad state (i.e., bit error rate is high) due to significant cyclic variations in the concentration of carbon dioxide in the channel. Using real res-

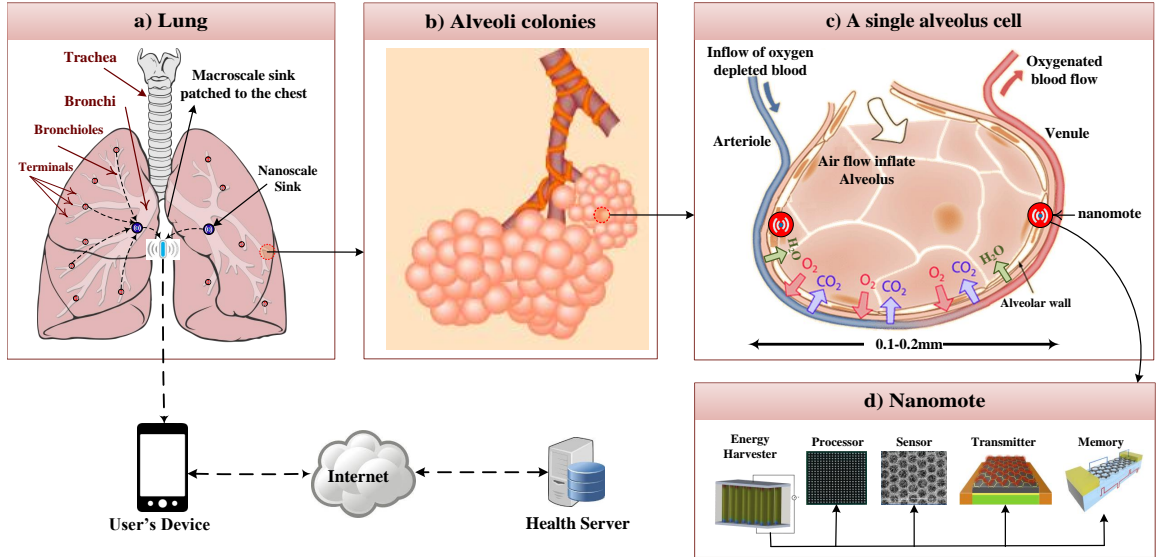


Figure 1: A schematic architecture of the proposed lung monitoring system via WNSN.

piratory data, we have shown that these channel variations are significant. More specifically, it takes 20x less power to communicate reliably if all communications are scheduled only during good channel states, which appear once in every 3 seconds, compared to the case when nanosensors communicate randomly at any time. Therefore, we propose duty cycling as a solution for nanomotes to smartly transmit only when the channel is good. Finally, we propose simple channel estimation algorithms that enable the nanosensors to achieve such scheduling.

The rest of the paper is structured as follows. The proposed WNSN for lung monitoring is presented in Section 2. The terahertz channel inside lung cells is analysed in Section 3 followed by the proposed duty cycling protocols in Section 4. We present simulation results in Section 5 and conclude the paper in Section 6.

2. PROPOSED WNSN FOR LUNG MONITORING

WNSNs are expected to sense and control important physical processes right at the molecule level delivering unprecedented performance improvement of medical, industrial, biological, and chemical applications [1, 17]. There are some indications that show WNSNs can potentially be deployed inside human body for different purposes such as health monitoring and targeted drug delivery systems [1, 3].

It is well-known that by monitoring the composition of the exhaled air, many diseases such as asthma, bronchiectases and even lung cancer can be detected at the very early stage of development [11]. For example, volatile organic compounds (VOCs) in breath are recently found as a novel biomarker that can provide precise information for quick diagnosis of the lung cancer [15].

In this work, we demonstrate using WNSNs to remotely monitor human lung at the molecular level. We first describe the lung structure followed by the proposed WNSN-based architecture for remote lung cell monitoring.

2.1 Lung Structure

The human lung is the organ of respiration, composed of a pair of large, spongy organs optimized for gas exchange between the blood and the air (Figure 1.a). Air enters the body through the nose or mouth and passes through the pharynx, larynx, and trachea. The trachea is a tube that connects the larynx to the bronchi of the lungs. Just before reaching the lungs, the trachea then splits into the left and right bronchi. Many small bronchioles branch off from the bronchi. The bronchioles further branch off into many tiny terminal bronchioles. Terminal bronchioles are the smallest air tubes in the lungs and terminate at the alveoli of the lungs, a colony of lung smallest cell that is called alveolus (Figure 1.b).

Alveolus cells are the functional units of the lungs that permit gas exchange between the air in the lungs and the blood in the capillaries of the lungs that have surrounded each alveolus cell (Figure 1.c). A thin layer of connective tissue underlies and supports the alveolar cells. The respiratory membrane is formed where the walls of a capillary touch the walls of an alveolus. At the respiratory membrane, gas exchange occurs between the air and blood through the extremely thin walls of the alveolus and capillary.

Upon inspiration, the intra-alveolar pressure change around 5-6 mmHg within one respiration cycle due to relaxation of the intercostal muscles and diaphragm. Due to the same reason, the radii of an alveolus periodically varies between about 0.1 mm to 0.2 mm. We will later use these variations to harvest energy for our nanomotes.

Now we describe our proposed WNSN-based architecture for real-time monitoring of human lung cells.

2.2 Proposed Architecture

The proposed system aims to measure and report few markers that can help to detect the lung-related diseases. We target sparse sampling from several alveoli colonies that have been selected across both left and right lungs. For this purpose, we propose a hierarchical WNSN-based solution

which includes four levels that has been depicted in Figure 1.

At the lowest level, we assume that we can deploy two nanomotes within each targeted alveolus cell to collect data from the cell. We refer to these nanomotes as ‘*nanocollectors*’. Nanocollectors can be attached to the cell walls by using some bioengineering techniques such as atomic force microscopy or some form of artificial bacteria [9]. Each nanocollector has been equipped with a nanoscale energy harvester [5] to harvest energy from pressure variation and cell wall movement during the respiration cycle ; a nanosensor [16] to measure the target markers in the exchanged gases; a nanomemory [13] to save the detected marker; a nanoprocessor [4] to run the required algorithm and a nanotransmitter [7] to transfer the recorded markers wirelessly to a nanoscale remote station. A schematic of the proposed nanocollector has been depicted in Figure 1.d.

In the next level, two nanoscale remote stations would be deployed in the central point of both left and right lungs that are able to receive signal from many nanocollectors. These nanoscale sinks which will be referred as ‘*nanosinks*’ have similar modules to nanocollector except they do not have any sensor but instead have an extra energy harvester that can scavenge energy from RF waves. Nanosinks can transmit the received data from the nanocollector to the next level which is a macroscale sink (*macrosink*) that has been patched to the external skin of the chest in a proper position that minimizes the distance between macrosink and the nanosinks. The macrosink then transmit the received data from nanosinks to the user device that could be a mobile phone or a personal computer. The data would be processed by a spacial software on the device and the results would be displayed on the user’s device monitor. For further analysis or to keep the person’s record on a cloud, the data could be remotely transferred to a health server via Internet.

2.3 Powering of nanomotes

The nanocollectors can use a piezoelectric nanogenerator to either harvest energy from the motion due to alveolus cell movement or pressure variation during the respiration process. According to the literature up to few pW (10^{-12}) can be harvested from motions of human organs using a flexible piezoelectric nanogenerator of one square micron size [5].

The nanosinks need more power as they need to collect data from many nanocollectors and transmit data to the macrosink. RF energy harvesting might be an option for nanosink, i.e. macrosink feed the nanosinks via wireless RF transmissions.

3. IN-VIVO THZ CHANNEL MODELLING

The small antenna size dictates that nanomotes operate over very high frequencies, namely the terahertz band [1, 7]. As terahertz band is the resonance frequency of molecules, communication in this band is severely affected by molecular absorption noise and attenuation.

Radio communication is affected by the chemical compositions of the medium in two different ways in the terahertz band. First, radio signal is attenuated because molecules in the channel absorb energy in certain frequency bands. Second, this absorbed energy is re-radiated by the molecules which creates noise in the channel. We assume that the radio channel is a medium consisting of N chemical species

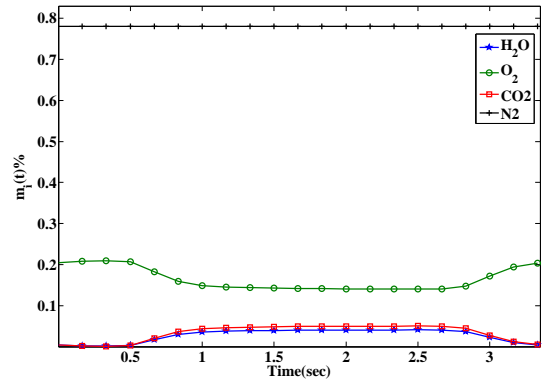


Figure 2: Alveoli gas composition during one respiration cycle.

S_1, S_2, \dots, S_N . The effect of each chemical species S_i on the radio signal is characterised by its molecular absorption coefficient $K_i(f)$ of species S_i at frequency f . The molecular absorption coefficients of many chemical species are available from the HITRAN database [2].

In this section, we aim to characterise the THz communication within human body based on radiative transfer theory presented in [6].

3.1 Human lung as the communication medium

As we mentioned in previous section, the quality of communication in WNSN is strongly affected by the composition of the communication medium. It is then important to identify the composition of the medium. In the proposed architecture in Section 2, we have three mediums including communication between nanocollectors within one alveolus cell; between nanocollectors and nanosinks; and between nanosink and macrosink. In this paper, we focus only on the first medium, i.e. communication within alveolus cells, which is the most challenging medium due to the dynamic nature of its composition arising from the respiration process. The communication between nanocollectors is mainly affected by the exchanged gases in the membrane of the alveolus cells which is modulated by the human respiratory system. In addition, the blood circulatory system circulates the blood through the body; carrying oxygen to the cells; collecting the excess water and CO₂ which has been produced during cell respiration; and carries them to the alveolus cells in the lungs (Figure 1.c). This process affects the composition of the alveolus cells. Table 1 shows the composition of the in/exhaled air. While less than 0.04% of the inhaled air is CO₂, the exhaled air is composed of 4-5 CO₂.

Table 1: The composition percentage of exhaled and inhaled air [10].

	N ₂	O ₂	CO ₂	H ₂ O	Others
Inhaled air	78	21	0.05	< 1	< 0.1
Exhaled air	78	13-16	4-5	3-5	< 0.1

Figure 3 shows the variation of the mole fraction, i.e. ratio of CO₂ during the respiration process in 10 second that contains 3 full respiration cycles for an adult person which

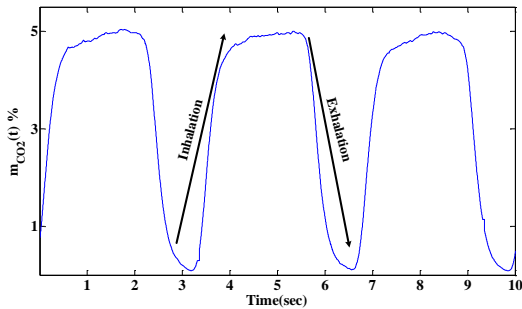


Figure 3: Variation of the CO₂ during the respiration in 10 second that has been experimentally measured [8].

has been obtained by real measurement [8]. It shows that CO₂ mole fraction fluctuated between 0.05-5 %. It starts at 0.05 at the beginning of inhalation and raises to around 5% at the end of inhalation. It drops again to 0.05 at the end of exhalation. Similar pattern has been observed in all respiration cycles. We use the data of Table 1 and the respiration data of the same person to simulate the gas exchange in the alveolus cell. Figure 2 shows the concentration (mole fraction) of different molecules during the gas exchange process in alveolus cell. As it can be seen, the composition of alveoli as our wireless medium is variable over time causing a time-varying WNSNs.

In the next section, we show how this variation in the composition of the medium can affect the quality of communication over the terahertz band.

3.2 Time-varying WNSN

We consider a radio channel in a medium which has time-varying chemical composition. Let $m_i(t)$ be the mole fraction of chemical species S_i in the medium at time t . The medium absorption coefficient $K(t, f)$ at time t and frequency f is a weighted sum of the molecular absorption coefficients in the medium:

$$K(t, f) = \sum_{i=1}^N m_i(t) \times K_i(f) \quad (1)$$

where $K_i(f)$ is the absorption coefficient of molecules i at the frequency f .

As we discussed in Section 3.1, Figure 2 shows the evolution of different molecules during the gas exchange process within one alveolus cell.

The attenuation at time t , frequency f and a distance d from the radio source is given in [6]:

$$A(t, f, d) = e^{K(t, f)d} \times \left(\frac{4\pi fd}{c} \right)^2 \quad (2)$$

where c is the speed of light. The molecular absorption noise, $N_{\text{abs}}(t, f, d)$, which is due to the re-radiation of absorbed radiation by the molecules in the channel, is given by [6]:

$$N_{\text{abs}}(t, f, d) = k_B T_0 (1 - e^{-K(t, f)d}) \quad (3)$$

where T_0 is the reference temperature 296K and k_B is the Boltzman constant.

Let $U(t, f)$ be the power spectral density of the transmitted radio signal at time t and frequency f . The signal-to-

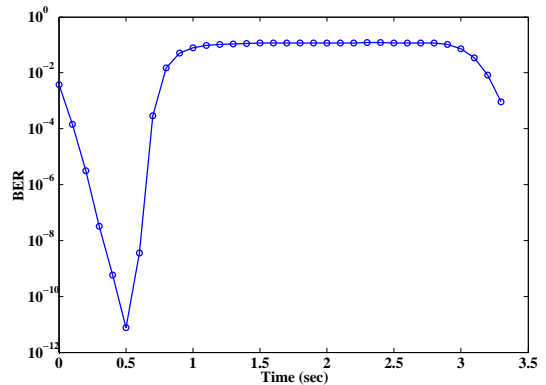


Figure 4: BER during one respiration cycle.

noise ratio (SNR) at time t , frequency f and distance d is:

$$\text{SNR}(t, f, d) = \frac{U(t, f)}{A(t, f, d)N_{\text{abs}}(t, f, d)} \quad (4)$$

3.3 Channel simulation

Now, we are ready to analyse the quality of communication within alveolar. We first calculate the SNR based on the procedure of Section 3. We then use Pulse Amplitude Modulation (PAM) to calculate the Bit Error Rate (BER). Figure 4 shows the BER of the medium in one respiration cycle. It shows the BER fluctuated over time as the medium is mainly affected by gas exchanged process.

In the next section, we introduce two smart communication protocols that can duty cycle the nanomote to smartly wake-up and transmit when the BER in the channel is low.

4. BIO-INSPIRED DUTY CYCLING COMMUNICATION PROTOCOLS

In Section 2, we described how a WNSN can be used to monitor the lung biomarkers at the molecular level for early detection of the related diseases. We also showed in Section 3 that the quality of communication (BER) among nanomotes is variable over time, which is due to variation in the composition of the medium that is modulated by the human respiratory system. There are two approaches to provide reliable communication in such time-varying WNSN's channel. First, nanomotes can use a constant high transmission power to overcome the worst possible absorption in the channel. This approach can guarantee a target BER in the channel but it wastes the power when the channel's absorption is low which is not appropriate for resource restricted nanomotes. The second approach is dynamic power allocation [19] in which the nanomotes continuously adjust their transmission powers proportional to the channel's state, i.e. absorption coefficient while maintaining a low overall power budget.

Although dynamic power allocation can improve the reliability of communication, compared to the constant power allocation approach, it is more appropriate for applications that need to collect real-time data samples at a very high rate. However, in our proposed lung monitoring system, we do not need to collect continuous samples, instead the sys-

tem requires to collect data at a low frequency, e.g. every few seconds. We therefore aim to design duty cycling protocols that smartly take advantage of the respiration information to transmit only when the channel's absorption is low. We will explain this protocol in the next Section.

4.1 Smart Sleep & Wake-up Protocol (SSW)

The aim of this section is to design a smart duty cycling protocol that allows nanomotes to intelligently stop transmitting when the absorption in the channel is high and only resume data transmission when the channel is good, i.e. the absorption is low. We refer to this protocol as smart sleep and wake-up (SSW) protocol. Let assume each respiration cycle $C(x)$ contains N discrete time slots:

$$C(x) = \{t_{x_1}, t_{x_2}, t_{x_3}, \dots, t_{x_N}\}$$

Then, $T_x = t_{x_N} - t_{x_1}$ is the duration of the respiration cycle. The wake-up period for respiration cycle $C(x)$, $\Delta T_W(x)$, define as the time slots that the channel has the lowest possible absorption during a given respiration cycle of $C(x)$:

$$\Delta T_W(x) = \{t_{x_i} \in C(x) \text{ and } \bar{K}(t_{x_i}) \leq \eta \times \Gamma(x); \eta \geq 1\} \quad (5)$$

where $\bar{K}(t)$ is the average absorption coefficient of the channel at time t that can be obtained from integration of Equation 1 over transmitter's bandwidth, $\Gamma(x)$ is the minimum average absorption coefficient in the channel over $C(x)$ and $\eta > 1$ is a design parameter. The sleep period of the nanomotes over cycle x , $\Delta T_S(x)$ would simply be:

$$\Delta T_S(x) = C(x) \setminus \Delta T_W(x)$$

Now, we explain how nanomotes can practically estimate $\Delta T_W(x)$ for a given respiration cycle of $C(x)$. As we described in Section 2, we have two nanocollectors in each alveolus cell. Both nanomotes run algorithm 1 for T_x second to calculate $\Delta T_W(x)$:

Algorithm 1: Wake-up intervals calculation.

```

 $\chi = \emptyset$ 
while  $t < T_x$  do
  Transmit an estimation packet.
  Measure the received SNR from the counterpart
  nanocollector and label it as  $\gamma_t$ .
   $\chi = \chi \cup \gamma_t$ 
   $t = t + \Delta t$  which  $\Delta t > 1ms$ 
 $\Delta T_W(x) = \{t \in T_x \text{ and } \gamma_t \geq \eta \times \min\{\chi\}\}$ 

```

SSW can offer the best sleep & wake-up cycle but it needs nanomote to know the exact duration of each individual respiration cycle, $C(x)$ and also the exact values for channel absorption or SNR over the entire cycle. For a given person, the average respiration rate depends on the age, gender, health condition and the activity that person is doing. Hence, the respiration cycle time, $C(x)$ can be approximated for a given person in a given health and activity condition. Nevertheless, continues real-time measuring of the SNR in the channel is not practical for resource restricted nanomotes as it will exhaust their limited energies and also might affect their functionalities. In the next section, we therefore propose a practical protocol that can approximate the wake-up

and sleep cycles based on only the real measurements from only one respiration cycle.

4.2 Extended Smart Sleep & Wake-up Protocol (ESSW)

Let assume that we can obtain the wake-up and sleep period for one respiration cycle via algorithm 1, $\Delta T_W(x)$. The extended SSW (ESSW) tries to extend this information to obtain the wake-up and sleep periods for all other respiration cycles.

Although for a given person p in a given condition, the exact period for each individual respiration cycle, $T_{p,x}$, is different but our investigation shows that the average period, \bar{T}_p has a small variance (less than 5%) which means it can be used as a good estimation for each individual cycle time. The wake-up period for other next respiration cycles would be:

$$\Delta T_W(x+i) = \Delta T_W(x) + i \times \bar{T}_p \quad (6)$$

where $\Delta T_W(x)$ is the calculated wake-up period for cycle x and \bar{T}_p is the average period for respiration cycles of the person p that can be obtained from the respiratory rate of the person.

Although the respiration period for a given person can be considered as fixed but if user changes his activity, e.g. starts walking prior to running, then the respiratory rate and as a result the cycle periods will change. Nanomotes therefore need to re-calibrate their \bar{T}_p parameter to have a realistic estimation for the wake-up/sleep periods. The estimation of period in different activities and re-calibration process is left for future work.

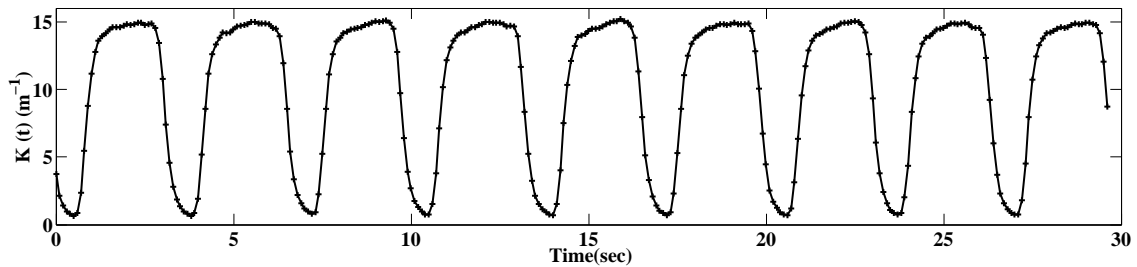
5. RESULTS

This section aims to study the performance of the smart communication protocols proposed in Section 4. A good protocol is the one which provides a higher reliability for a given power budget. We compare two proposed protocols, SSW and ESSW against a *default* power allocation policy that use a constant power allocation all the time.

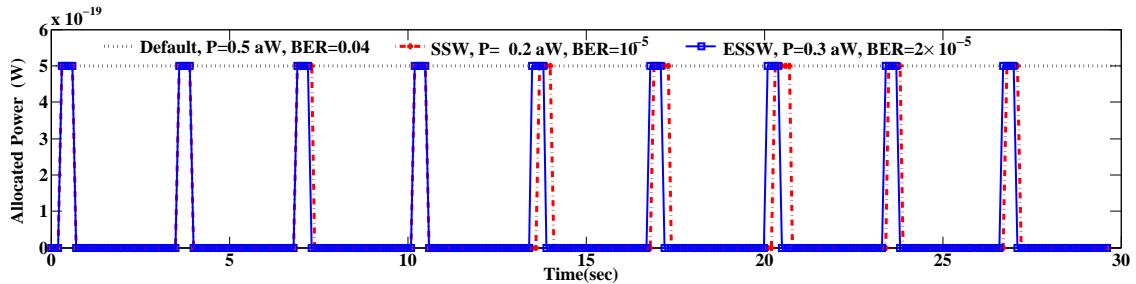
5.1 Methodology

We consider a single hop communication between two nanomotes that are communicating within an alveolus medium over a distance equal to 0.2mm. We extract the respiration data from CapnoBase database [8] for an adult person with respiratory rate of 18 breaths per minutes for 30 second that includes 9 respiration cycles, each around 3.32 second (T_x). Then, we follow the same steps as in Section 3.3 to simulate the gas exchange process in alveolus cells in each of 9 cycles, i.e. we extract the mole fractions of different molecules to calculate $K(t)$. Then, in order to implement SSW protocol, we follow the algorithm 1 with $\eta = 2$ to calculate the wake-up periods for all 9 cycles $\Delta T_W(x_1), \dots, \Delta T_W(x_9)$. We also use the first wake-up period, $\Delta T_W(x_1)$ to approximate other 8 wake-up periods from equation 5 for ESSW. Finally, we use the WNSN's channel modelling described in Section 3 to calculate SNR and BER for each protocol/cycle.

For each protocol/cycle, we conduct 30 sets of experiments, each with a different nominal power levels, P_{nominal} that is ranging from 10^{-19} to 10^{-17} W that are equally spaced. For default power allocation, each nanomote uses P_{nominal} as the transmission power all the time. For other



(a) Average absorption coefficient of the channel



(b) Power allocation via default, SSW and ESSW.

Figure 5: Channel status and power allocation via different protocols within alveolus medium over 9 respiration cycles (nominal power equal to 0.5 aW).

policies, nanomote use P_{nominal} only during the wake-up periods and use $P_{\text{nominal}} = 0$ during the sleep period, i.e. don't transmit. The average allocated power over each cycle via each protocol therefore would be P_{nominal} for default protocol and $\frac{\Delta T_W(x)}{T_x} \times P_{\text{nominal}}$ for SSW and ESSW. Note that $\Delta T_W(x)$ for SSW and ESSW might be slightly different due to estimation error.

5.2 Results

Figure 5.a illustrates the $\bar{K}(t)$ over 9 respiration cycles. It shows that absorption coefficient of the alveolus channel varies between 1 and 15 m^{-1} . Figure 5.b shows the typical power allocation via 3 different protocols over the 9 cycles for a nominal power equal to 0.5aW (0.5×10^{-18}). As it can be seen, the SSW can successfully capture the moments that absorption is low in the channel. ESSW which uses the wake-up period of the first cycle to estimate other wake-up periods is also relatively close to the SSW. While default protocol uses 0.5 aW to provide BER of only 0.04, SSW and ESSW can improve the BER to 10^{-5} and 2×10^{-5} by spending almost half of the power that default protocol has used.

Figure 5 shows the results for a given nominal power. Now, let investigate the performance of proposed protocols when nanomotes use different nominal powers. Figure 6 shows the power/BER trade-off for different protocols. It shows that for a given power budget, the SSW can significantly improve the BER of the default protocol by few orders of magnitudes. On the other hand, for a given BER, SSW and ESSW reduce the required power by a factor of averagely 20 and 18, compared to the default protocol. We hypothesize that this lower performance of the ESSW is due to the variation in the respiration times, T_x which has been considered fixed in equation 5.

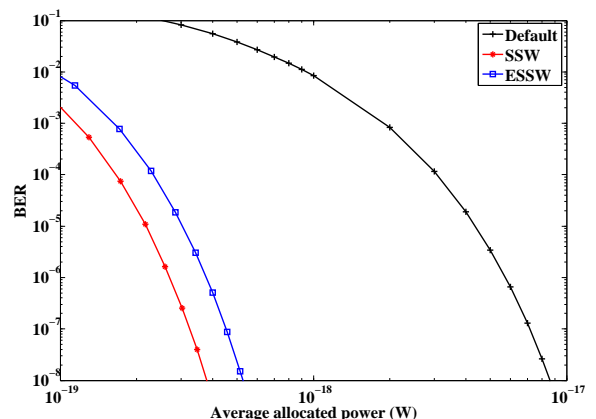


Figure 6: Achievable BER via different protocols as a function of average allocated power for the alveolus medium.

As the SSW and ESSW only transmit over a fraction of respiration cycle, it might negatively affect the channel capacity. So, we use the Shannon capacity formula [6] to calculate the average achievable channel capacity for different protocols over one respiration cycle that has been presented in Figure 7. Although SSW and ESSW have a relatively long sleep cycle, which means their capacities are zero, but they performs better than default protocol as their average SNR over wake-up period is significantly higher than the average SNR of the default protocol over the entire cycle. For fair comparison, we consider zero capacity for SSW and ESSW during the sleep cycles.

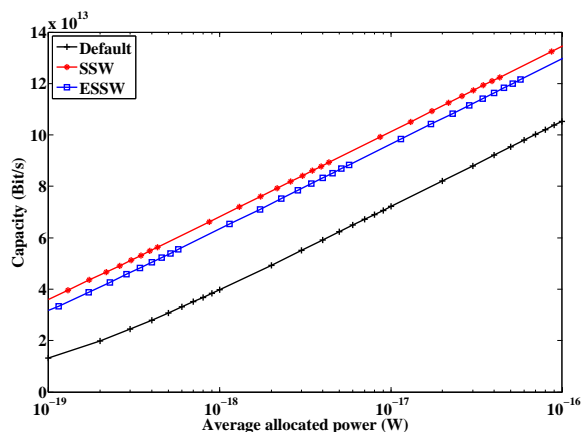


Figure 7: Capacity of different protocols as a function of average allocated power in alveolus medium.

6. CONCLUSION

We have presented the concept of a WSN for monitoring human lung cells. Using radiative transfer theory, we have studied the characteristics of terahertz communication channels that may be encountered in human lungs. The key finding is that the respiration process is the major factor that influences the terahertz channel inside lung cells. The channel periodically switches between good and bad states due to significant cyclic variations in the concentration of the exchanged gases in the human lung. Using real respiratory data, we have shown that these channel variations are significant. More specifically, it takes 20x less power to communicate with a low BER less than 10^{-6} if communication is restricted to good channel states than the case where this restriction is not enforced. Given that good channel states cyclicly reappear once every 3 seconds, the power saving, which directly reduces the electromagnetic radiation in lung cells, can still support high frequency monitoring. We have further shown that it is possible for nanosensors to accurately detect and predict the timings of good and bad channel states, making the power saving viable.

7. REFERENCES

- [1] I. F. Akyildiz and J. M. Jornet. Electromagnetic wireless nanosensor networks. *Nano Communication Networks*, 1(1):3–19, Mar. 2010.
- [2] Y. L. Babikov, I. E. Gordon, and S. N. Mikhailenko. "HITRAN on the Web", a new tool for HITRAN spectroscopic data manipulation. In *The proceeding of the ASA-HITRAN Conference*, Reims, FRANCE, 2012.
- [3] F. Dressler and S. Fischer. Connecting in-body nano communication with body area networks: Challenges and opportunities of the internet of nano things. *Nano Communication Networks*, 6(2):29 – 38, 2015.
- [4] M. Fuechsle, J. a. Miwa, S. Mahapatra, H. Ryu, S. Lee, O. Warschkow, L. C. L. Hollenberg, G. Klimeck, and M. Y. Simmons. A single-atom transistor. *Nature nanotechnology*, 7(4):242–6, Apr. 2012.
- [5] G.-T. Hwang, M. Byun, C. K. Jeong, and K. J. Lee. Flexible piezoelectric thin-film energy harvesters and nanosensors for biomedical applications. *Advanced Healthcare Materials*, 4(5):646–658, 2015.
- [6] J. Jornet and I. Akyildiz. Channel modeling and capacity analysis for electromagnetic wireless nanonetworks in the terahertz band. *IEEE Transactions on Wireless Communications*, 10(10):3211–3221, 2011.
- [7] J. Jornet and I. Akyildiz. Graphene-based plasmonic nano-antenna for terahertz band communication in nanonetworks. *Selected Areas in Communications, IEEE Journal on*, 31(12):685–694, December 2013.
- [8] W. Karlen, S. Raman, J. M. Ansermino, and G. A. Dumont. Multiparameter respiratory rate estimation from the photoplethysmogram. *IEEE transactions on bio-medical engineering*, 60(7):1946–53, 2013.
- [9] S. Lenaghan, Y. Wang, N. Xi, T. Fukuda, T. Tarn, W. Hamel, and M. Zhang. Grand challenges in bioengineered nanorobotics for cancer therapy. *Biomedical Engineering, IEEE Transactions on*, 60(3):667–673, March 2013.
- [10] W. J. P. D. Marshall and S. K. Bangert. *Clinical chemistry*. Edinburgh ; New York : Mosby, 5th ed edition, 2004. Includes index.
- [11] P. J. Mazzone, X.-F. Wang, Y. Xu, T. Mekhail, M. C. Beukemann, J. Na, J. W. Kemling, K. S. Suslick, and M. Sasidhar. Exhaled breath analysis with a colorimetric sensor array for the identification and characterization of lung cancer. *J Thorac Oncol*, 7(1):137–142, Jan 2012.
- [12] J. Riu, A. Maroto, and F. Rius. Nanosensors in environmental analysis. *Talanta*, 69(2):288–301, 2006.
- [13] E. U. Stutzel, M. Burghard, K. Kern, F. Traversi, F. Nichele, and R. Sordan. Data storage: A graphene nanoribbon memory cell. *Small*, 6(24):2821–30, 2010.
- [14] G. von Maltzahn, J.-H. Park, K. Y. Lin, N. Singh, C. Schweppe, R. Mesters, W. E. Berdel, E. Ruoslahti, M. J. Sailor, and S. N. Bhatia. Nanoparticles that communicate in vivo to amplify tumour targeting. *Nat Mater*, 10(7):545–552, Jul 2011.
- [15] C. Wang, R. Dong, X. Wang, A. Lian, C. Chi, C. Ke, L. Guo, S. Liu, W. Zhao, G. Xu, and E. Li. Exhaled volatile organic compounds as lung cancer biomarkers during one-lung ventilation. *Sci. Rep.*, 4, Dec 2014.
- [16] C. R. Yonzon, D. a. Stuart, X. Zhang, and A. D. McFarland. Towards advanced chemical and biological nanosensors-An overview. *Talanta*, 67(3):438–48, 2005.
- [17] E. Zarepour, A. A. Adesina, M. Hassan, and C. T. Chou. Innovative approach to improving gas-to-liquid fuel catalysis via nanosensor network modulation. *Industrial and Engineering Chemistry Research*, 53(14):5728–5736, 2014.
- [18] E. Zarepour, M. Hassan, C. T. Chou, A. Adesina, and M. Ebrahimi. Reliability analysis of time-varying wireless nanoscale sensor networks. In *the proceedings of 15th IEEE Conference on Nanotechnology (IEEE-NANO)*, Rome, Italy, July 2015.
- [19] E. Zarepour, M. Hassan, C. T. Chou, and A. A. Adesina. Power Optimization in Nano Sensor Networks for Chemical Reactors. In *the proceedings of ACM International Conference on Nanoscale Computing and Communication*, Atlanta, Georgia, USA, 2014.